[CANCER RESEARCH 64, 678–688, January 15, 2004]

Novel Mode of Action of Tylophorine Analogs as Antitumor Compounds

Wenli Gao,[1] Wing Lam,[1] Sanbao Zhong,[2] Conrad Kaczmarek,[2] David C. Baker,[2] and Yung-Chi Cheng[1]

[1]Department of Pharmacology, Yale University School of Medicine, New Haven, Connecticut, and [2]Department of Chemistry, The University of Tennessee, Knoxville, Tennessee

ABSTRACT

Tylophorine and its analogs are phenanthroindolizidine alkaloids, several of which have been isolated from the *Tylophora* genus of plants. Evaluation of (+)-*S*-tylophorine [DCB-3500 (NSC-717335)] and its analog DCB-3503 (NSC-716802) in the National Cancer Institute tumor screen showed a fairly uniform and potent inhibition of cell growth in all 60 cell lines (GI_{50} $\sim 10^{-8}$ M). To further evaluate the antitumor potential of these compounds, we synthesized four tylophorine analogs, designated DCB-3500, DCB-3501, DCB-3502, and DCB-3503. All four tylophorine analogs exerted potent growth-inhibitory effects against HepG2, a human hepatocellular carcinoma cell line, and KB, a human nasopharyngeal carcinoma cell line. HepG2 cells were more sensitive than KB in terms of loss of clonogenicity. KB variants, which are resistant to etoposide, hydroxyurea, or camptothecin, have similar sensitivities to the tylophorine analogs, as do the parental KB cells. Treatment of nude mice bearing HepG2 tumor xenografts by i.p. injections of DCB-3503 at 6 mg/kg every 8 h on days 0 and 3 resulted in significant tumor growth suppression ($P < 0.0001$). Unlike conventional antitumor drugs, 3 μM DCB-3503 did not cause DNA breaks or apoptosis in HepG2 cells. Tylophorine analogs induced albumin expression and decreased α-fetoprotein expression in HepG2 cells, which suggests that tylophorine analogs could induce HepG2 differentiation. Tylophorine analogs had an inhibitory effect on cyclic AMP response elements, activator protein-1 sites, or nuclear factor-κB binding site-mediated transcriptions. In summary, these tylophorine analogs are a unique class of antitumor compounds that have a mode of action different from known antitumor drugs.

INTRODUCTION

(+)-(*S*)-Tylophorine and its analogs are phenanthroindolizidine alkaloids, many of which have been isolated from plants of the family Asclepiadaceae, including members of the genus *Tylophora* that are native to India and Southeast Asia (1). These compounds, commonly referred to as tylophora alkaloids, because of their reported antitumor activity (1–8), have been the targets of synthesis, modification, and antitumor evaluation in our laboratories. Evaluation of (+)-(*S*)-tylophorine [DCB-3500 (NSC-717335)] and its analog DCB-3503 (NSC-716802) in the antitumor screen at the National Cancer Institute showed a fairly uniform and potent growth-inhibitory activity (GI_{50}, $\sim 10^{-8}$ M) in all 60 cell lines, with notable selectivity toward several refractory cell lines, including melanoma and lung tumor cell lines based on LC_{50} values (concentration of drug resulting in a 50% reduction in the measured protein at the end of the drug treatment as compared with that at the beginning). COMPARE analysis (9) showed their activity to be unique among known antitumor compounds, suggesting a mode of action that is distinctly different from other cancer chemotherapeutic compounds.[3]

Although the National Cancer Institute (NCI) tumor screen does not include hepatoma cell lines, our laboratory has maintained an interest in hepatocellular carcinoma (HCC) because it is common in Asia and its incidence is increasing in the United States (10). Thus far, there is no effective chemotherapy, and surgery remains the only potential cure (11). The 5-year survival rate of HCC is <5% (10). To this end, our laboratory has been interested in screening compounds that may have the potential to treat HCC. Most current antitumor chemotherapeutic drugs exert their action by induction of DNA breaks, inhibition of DNA synthesis, or perturbation of tubulin function. Compounds with new mechanisms of action are needed for the treatment of refractory cancers such as HCC. In view of the novel properties of this class of compounds suggested by the NCI study, we tested whether tylophorine analogs have potential antitumor activity against a HCC cell line, HepG2.

One of the major problems with cancer chemotherapy is drug resistance. Among the best characterized mechanisms of drug resistance is the overexpression of the multidrug resistance gene (mdr) product, 170-kDa P-glycoprotein (12, 13), or the 190-kDa multidrug resistance protein, MRP (14). Both are ATP-binding cassette transport proteins that actively pump the drugs out of the cell, leading to drug resistance. Other mechanisms, such as decreased expression of topoisomerase I or II, could render cells resistant to topoisomerase-targeting poisons (15, 16). Recently, antiapoptotic proteins have been shown also to play a role in drug resistance. For instance, activation of nuclear factor (NF)-κB has been suggested as one of the mechanisms of resistance to chemotherapy because of its antiapoptotic role (17, 18). In view of the refractory nature of HCC as caused by these known mechanisms of drug resistance, an effective compound against HCC ideally would not be susceptible to these mechanisms.

Signaling pathways, which play important roles in cell proliferation, differentiation, and survival, represent exciting targets for developing new antitumor drugs. We are currently witnessing clinical successes resulting from this targeting approach, exemplified by imatinib (STI-571; Gleevec), a specific Bcr-Abl tyrosine kinase inhibitor (19), approved recently by the Food and Drug Administration for chronic myelogenous leukemia. Screening for NF-κB inhibitors is another actively exploited area (20). NF-κB is a key transcription factor initially discovered and demonstrated to be involved in immunological and inflammatory responses (21). Accumulating evidence suggests that NF-κB activity is associated with increased tumor cell survival, and conversely, suppression of NF-κB activity leads to a stimulation of an apoptotic response (22). PS-341 (bortezomib), a potent NF-κB inhibitor, is a lead compound in this class of drugs and was very recently approved by the Food and Drug Administration for the treatment of patients with refractory multiple myeloma (23).

In this report, we investigated the potential antitumor activity of tylophorine analogs against hepatocellular carcinoma both *in vitro* and *in vivo* and further tested the effects of these compounds on diverse cellular events, such as cell cycle, apoptosis, senescence, and differentiation. The impact of tylophorine analogs on key signaling pathways was also investigated.

MATERIALS AND METHODS

Materials. Cell culture medium, fetal bovine serum, and G418 were purchased from Invitrogen. FuGENE6 transfection reagent was from Roche.

Received 6/27/03; revised 10/21/03; accepted 11/10/03.

Grant support: NIH Grant R01 CA87863.

The costs of publication of this article were defrayed in part by the payment of page charges. This article must therefore be hereby marked *advertisement* in accordance with 18 U.S.C. Section 1734 solely to indicate this fact.

Notes: W. Gao and W. Lam contributed equally to this work. Y-C. Cheng is a Fellow of the National Foundation for Cancer Research.

Requests for reprints: Yung-Chi Cheng, Department of Pharmacology, Yale University School of Medicine, 333 Cedar Street, New Haven, CT 06510. Phone: (203) 785-7119; Fax: (203) 785-7129; E-mail: cheng.lab@yale.edu.

[3] Access to the 60-cell line NCI test data, along with *in vivo* data and a protocol to run COMPARE analysis, can be accessed from the NSC numbers at the following Web site: http://dtp.nci.nih.gov/dtpstandard/dwindex/index.jsp.

β-L-(−)-Dioxolane cytidine (L-OddC) was provided by Dr. C. K. Chu (University of Georgia, Athens, GA). Standard chemotherapeutic agents, etoposide (VP-16), taxol, hydroxyurea, nocodazole, gemcitabine, camptothecin as well as forskolin, 12-*O*-tetradecanoylphorbol 13-acetate (TPA), and tumor necrosis factor α (TNF-α) were purchased from Sigma-Aldrich (St. Louis, MO) and Calbiochem (San Diego, CA). Tylophorine analogs DCB-3500 (NSC-717335), DCB-3501, DCB-3502, and DCB-3503 (NSC-716802) were synthesized in Dr. Baker's laboratory. These compounds were shown by high-pressure liquid chromatography, nuclear magnetic resonance spectroscopy, and mass spectrometry to be at least 98% pure (data not shown).[4]

Plasmids. Firefly luciferase reporter vectors pAP1-luc and pCRE-luc were purchased from Clontech, Mercury pathway profiling system. pBIIX-luc (containing two tandemly repeated NF-κB binding sites) was kindly provided by Dr. Ghosh (Yale University). pcDNA 3.1(+) was purchased from Invitrogen. *Renilla* luciferase reporter vector phRL was purchased from Promega.

Cell Culture. The human hepatocellular carcinoma cell lines HepG2, SK-Hep1, Huh7, PLC/PRF5, Hep3B, HA22T, Mahlavu, and the human nasopharyngeal carcinoma KB cells were maintained in RPMI 1640 supplemented with 10% fetal bovine serum. KB-resistant cell lines, KB-MDR, KB-7D, KB-7D-Rev, KB-Hu-R, KB-Hu-Rev, KB-100, and KB-100-Rev have been described before (24–29).

Cytotoxicity Assay. Cells (1×10^4/well) were plated in 24-well plates. After 24 h, cells were treated with drugs for three doubling times and then fixed and stained with 0.5% methylene blue (30) in 50% ethanol for 2 h, followed by washing with tap water to remove excess color. Plates were dried and then resuspended in 1% sarkosyl and rotated at room temperature for 3 h. Cell growth was quantitated based on the amount of methylene blue adsorbed to the cells as measured by a spectrophotometer (Molecular Devices) at 595 nm. EC_{50} was defined as the concentration of drug that inhibited cell growth by 50% after continuous drug exposure for three doubling times. All experiments were performed in triplicate wells and were repeated at least three times.

Clonogenic Assay. Cells (5×10^4/well) were plated in 6-well plates. After 24 h, cells were exposed to serial dilutions of drugs for 24 h. Cells were then trypsinized and counted, and cell viability was determined by trypan blue staining. Two hundred viable cells were plated in triplicate in 6-well plates and grown for 8–10 generations and then fixed and stained with 0.5% methylene blue in 50% ethanol for 1 h. After plates were washed and dried, the colonies were counted to obtain a cloning efficiency for each drug concentration. The CC_{50} was defined as the concentration of drug that produced a 50% decrease in cloning efficiency after 24-h drug exposure.

Animal Studies. Male NCr-nude mice (average body weight of 20 g), 4 weeks of age, were obtained from Taconic Farms Inc. and acclimated to laboratory conditions 1 week before tumor implantation. Nude mice were maintained in accordance with the Institutional Animal Care and Use Committee procedures and guidelines. Human HepG2 tumor xenografts were established by injecting s.c. 8×10^6 HepG2 cells. Treatment was initiated when the tumors were 100–250 mm^3, which is around 10 days after injection of HepG2 cells. DCB-3500 and DCB-3503 were dissolved in 0.5% DMSO; 0.5% Tween 80 in PBS and solvent alone served as control. DCB-3500, DCB-3503, and control vehicle were administered by i.p. injections. HepG2 tumors were measured daily using a caliper, and the body weights of the mice were monitored for toxicity. Tumor volume was estimated by using the formula length $\times$ width^2 $\times$ $\pi/6$.

Cell Cycle Analysis. KB and HepG2 cells were treated for 24 h with increasing concentrations of DCB-3500 and DCB-3503. At the end of treatment, cells were trypsinized, and the resulting cell suspensions were centrifuged at 1000 rpm for 5 min. The cells were fixed overnight in 70% ethanol at 4°C and centrifuged at 1000 rpm for 5 min, and the pellets were washed twice with ice-cold PBS. Cell pellets were then resuspended in 0.5 ml of PBS containing 50 μg/ml propidium iodide (Sigma-Aldrich) and 100 μg/ml RNase A (Sigma-Aldrich), incubated at 37°C for 30 min, and then analyzed by flow cytometer (Becton Dickson, Franklin Lakes, NJ). Data were analyzed using Modfit LT version 5.2 software (Verity Software House, Topsham, ME) for cell cycle profile.

Apoptosis Assay. Early apoptotic events were determined by using a Vybrant apoptosis assay kit (V-13241; Molecular Probes, Eugene, OR) according to the manufacturer's instructions. Briefly, control or treated cells were resuspended in Annexin binding buffer to $\sim 1 \times 10^6$ cells/ml, then stained with Alexa Fluor 488 Annexin V and/or propidium iodide (PI), and further incubated at room temperature for 15 min. Several controls were used to optimize instrument settings and determine gating windows. Negative controls were untreated, unstained cells and treated, unstained cells. Positive controls were cells treated with 3.7% formaldehyde for 15 min. These cells were found to bind both Annexin V and PI. They were divided into four aliquots: unstained; stained with Alexa Fluor 488 Annexin V alone; stained with PI alone; and double stained. Negative control cells and positive control cells were then analyzed by flow cytometer. Single stained with Annexin V was used as a positive control to set the apoptotic window. Single stained with PI was used as a positive control to set the necrotic window. Double-stained, formaldehyde-treated cells were mainly necrotic. Samples were then analyzed by flow cytometer under this condition. Acquired data were analyzed using WinMDI version 2.8 software.

Cell Growth Inhibition Assay. Cells (1×10^4/well) were plated in 6-well plates. After 24 h, cells were treated with drugs for another 24 h. The drug-containing medium was then removed, this time point was designated as day 0, and the cells were incubated in drug-free medium for another 1–8 days. At the end of each incubation period, cells were fixed and stained with 0.5% methylene blue in 50% ethanol and resuspended in 1% sarkosyl. The cell growth was quantitated as described in the cytotoxicity assay.

Confocal Microscopy. The confocal microscopic analysis was performed using methods similar to those described previously (29). Briefly, 5×10^4 HepG2 and KB cells were plated onto 22 × 22-mm glass coverslips in 35-mm culture dishes. After 24 h, cells were treated as indicated for another 24 h, and then drugs were taken away; this time point was designated as day 0. To monitor the expression levels of α-fetoprotein (AFP) and albumin, the cells were incubated in drug-free medium for another 2, 4, 5, 6, and 8 days. At the end of each incubation, cells were fixed with 4% paraformaldehyde at room temperature for 30 min, permeabilized by 0.5% Triton X-100 in PBS at room temperature for 15 min, and then incubated with 3% BSA in PBS at 4°C overnight to block nonspecific binding. Cells were further incubated with a monoclonal p53 antibody (1:100, Ab-2; Oncogene), a polyclonal AFP antibody (1:100, Ab-2; Lab Vision), or a monoclonal albumin antibody (1:100, Clone HSA-11; Sigma) at room temperature for 1 h, followed by FITC-conjugated anti-rabbit or anti-mouse IgG at 1: 100 dilution. Cytoplasm was counterstained with 0.25 μg/ml of rhodamine phalloidin (Molecular Probes, Eugene, OR). Cells were then sealed in antifade reagent (Molecular Probes). Confocal micrographs were scanned by a laser scanning confocal microscope, LSM 510 (Carl Zeiss, Inc., Thornwood, NY).

Western Blotting. HepG2 cells (5×10^5) were plated onto 6-well plates. After 24 h, cells were treated as indicated in the figure legends. To analyze extracellular signal-regulated kinase (ERK) 1/2 activity, cells were serum starved for 24 h before treatment. Cells were lysed in 2× SDS sample buffer (62.5 mM Tris-HCl, 2% SDS, 10% glycerol, 50 mM DTT, and 0.05% bromphenol blue) and sonicated 10 s to shear DNA. The whole-cell extracts were then electrophoresed through 12% SDS-polyacrylamide gels and transferred to nitrocellulose membranes (Amersham). The membranes were stained with Ponceau S to confirm equal protein loading and transfer. They were then incubated overnight at 4°C with blocking solution (TBS, 0.1% Tween 20, and 5% nonfat milk), followed by a specific antibody to p53 (1:500, mouse monoclonal antibody, Ab-2; Oncogene). To analyze ERK1/2 activity, the membranes were probed with a specific phospho-ERK1/2 (Thr-202/Tyr-204) antibody (1: 1,000, mouse monoclonal antibody; Cell Signaling). The membranes were then further incubated with horseradish peroxidase-conjugated anti-mouse IgG (1: 10,000; Sigma), and signals were visualized by enhanced chemiluminescence (Perkin-Elmer Life Science) as recommended by the manufacturers. The p53 blots were reprobed with antibodies to p21 (1:2,000, rabbit polyclonal antibody, kindly provided by Dr. Hui Zhang, Yale University) and actin (1: 2,000, mouse monoclonal antibody; Sigma). Phospho-ERK1/2 blots were reprobed with an ERK1/2 antibody (1:100, rabbit polyclonal antibody, Ab-2; Calbiochem).

Transfection and Luciferase Assay. HepG2 cells were plated at a density of 2×10^4 per well (48-well plate) and transfected with 0.2 μg of firefly luciferase reporter vector pAP1-luc, pCRE-luc, or pBIIX-luc, respectively, along with 20 ng of internal control vector, promoterless *Renilla* luciferase reporter vector phRL (Promega), using FuGENE6 transfection reagent accord-

[4] Synthesis and characterization, along with limited stability studies of the synthetic analogs, are to be published in a separate paper.

ing to the manufacturer's instructions. After 20 h, the medium was changed, and the cells were treated as indicated in the figure legends. Cell extracts were prepared, and luciferase activity was measured using a Dual-luciferase (firefly and *Renilla* luciferase) assay kit (Promega) according to the manufacturer's instructions. All transfection experiments were performed at least three times.

Generation of Stably Transfected Cell Lines. 1×10^6 cells per 100-mm dish were cotransfected with luciferase reporter vector pBIIX-luc and pcDNA3.1(+) at a molar ratio of 20:1 using FuGENE6 transfection reagent. Stable transfectants were selected with G418 (800 μg/ml), and individual colonies were transferred to 24-well dishes. Positive clones were screened by luciferase assay using a luciferase assay kit according to the manufacturer's instructions (Promega Luciferase Reporter 1000 assay system). Positive clones were maintained in the presence of 400 μg/ml of G418.

Statistical Analysis. Tumor volume data were analyzed using two-way ANOVA (GraphPad Prism 4, San Diego, CA). Student's *t* test (Microsoft Excel), and one-way ANOVA (GraphPad Prism 4) were used to examine the significance of other data. The difference was considered to be statistically significant when $P < 0.05$.

Table 1 *Growth inhibition and loss of clonogenicity of KB (human nasopharyngeal carcinoma) and HepG2 (hepatocyte carcinoma) cells*[a]

A. EC_{50}[b] (growth inhibition)

Cell line	DCB-3500 (nM)	DCB-3501 (nM)	DCB-3502 (nM)	DCB-3503 (nM)
KB	12 ± 3	106 ± 84	234 ± 91	28 ± 4
HepG2	11 ± 4	110 ± 45	264 ± 115	35 ± 5

B. CC_{50}[c] (colony-forming ability)

Cell line	DCB-3500 (μM)	DCB-3501 (μM)	DCB-3502 (μM)	DCB-3503 (μM)
KB	0.83 ± 0.31	3.07 ± 1.17	6.29 ± 3.74	1.55 ± 0.47
HepG2	0.04 ± 0.006	0.21 ± 0.13	0.45 ± 0.13	0.17 ± 0.08

[a] Values are means ± SD of three experiments, with each data point done in triplicate.
[b] Statistical analyses (one-way ANOVA and two-way ANOVA) showed that there was a significant difference between drugs ($P < 0.05$) but no significant difference between cell lines ($P = 0.14$).
[c] Statistical analyses (one-way ANOVA and two-way ANOVA) showed that there was a significant difference between drugs ($P < 0.05$), and there was an extremely significant difference between cell lines ($P < 0.0001$).

RESULTS

Tylophorine and Its Analogs Exert Potent Growth-inhibitory Effects on Both HepG2 and KB Cells. To explore the antitumor potential of tylophorine analogs, four compounds, DCB-3500, DCB-3501, DCB-3502, and DCB-3503, were synthesized. Their structures are shown in Fig. 1. DCB-3500 was synthesized and shown to be cytotoxic (2–3). DCB-3501 and DCB-3503 have been synthesized previously (31), but their biological activity has not been reported. DCB-3502 is novel in terms of structure. To test their stability, these compounds were observed in solution of 0.001 M phosphate buffer at pH 6.8 at room temperature in the dark and determined to be essentially stable for 12 h. Compounds were solubilized in methanol with a pH of 5.5. The integrity and concentration of these drugs were confirmed by high-pressure liquid chromatography before experiments were conducted.

The effects of these drugs on cell growth in KB cells and HepG2 cells were examined. Both cell lines were exposed to increasing concentrations of drugs, and dose-dependent growth inhibition was observed. As shown in Table 1*A*, the EC_{50}s of DCB-3500, DCB-3501, DCB-3502, and DCB-3503 for KB cells were determined to be 12 ± 3 nM, 106 ± 84 nM, 234 ± 91 nM, and 28 ± 4 nM, respectively. The EC_{50}s of DCB-3500, DCB-3501, DCB-3502, and DCB-3503 for HepG2 cells were determined to be 11 ± 4 nM, 110 ± 45 nM, 264 ± 115 nM, and 35 ± 5 nM, respectively. The EC_{50}s of these drugs were not significantly different ($P = 0.14$) between KB and HepG2 cells, but there was significant difference between drugs ($P < 0.05$). In addition, the EC_{50}s of DCB-3503 in other hepatoma cell lines SK-Hep1, Huh7, PLC/PRF5, Hep3B, HA22T, and Mahlavu were determined to be 19 ± 1 nM, 19 ± 6 nM, 25 ± 17 nM, 50 ± 29 nM, 80 ± 68 nM, and 82 ± 47 nM, respectively. Statistical analysis (one-way ANOVA) showed no significant difference between these data. We then measured the effects of the four tylophorine analogs on colony-forming ability of HepG2 and KB cells. As shown in Table 1B, CC_{50} of DCB-3500 was around 0.83 μM in KB cells and 0.04 μM in HepG2 cells, indicating that HepG2 cells were ~20-fold more sensitive than KB cells in terms of loss of clonogenicity in response to DCB-3500 treatment. Similar differential sensitivity was observed with the other compounds shown in Table 1B. On the basis of the observation that DCB-3500 and DCB-3503 were the most potent at inhibiting cell growth and reducing colony-forming ability, we focused our studies on these two compounds.

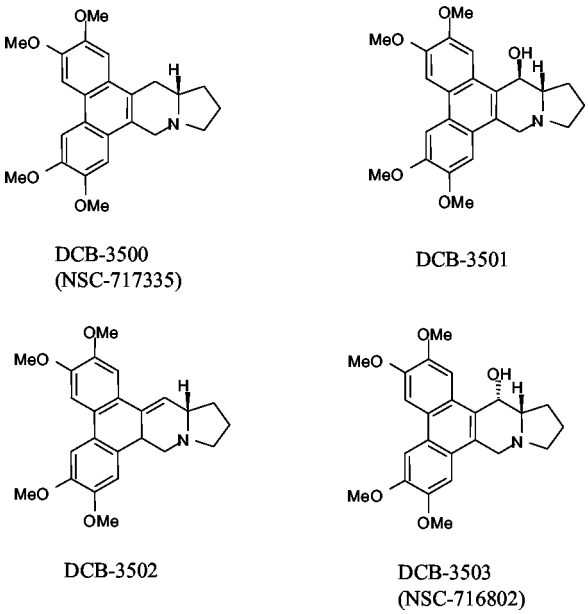

Fig. 1. Chemical structures of tylophorine analogs.

Antitumor Activity of Tylophorine and Its Analogs on Human HepG2 Tumor Xenografts. DCB-3500 and DCB-3503 were examined previously by the NCI for antitumor activity against 12 human tumor cell lines *in vivo* with a hollow-fiber assay (32, 33). The compound DCB-3503 showed excellent activity,[5] with a combined score of 26 (i.p., 16; s.c., 10), which ranks it among promising leads, according to the NIH protocol (32, 33). A lower combined score of 4 was found for DCB-3500. The fact that the latter showed much less activity might be caused by a drug delivery problem or lack of compound stability under experimental conditions over which we had no control. To further assess the therapeutic effect of DCB-3500 and DCB-3503 *in vivo*, animal studies were carried out using nude mice with HepG2 tumor xenografts. At 60 mg/kg, three times per day for 1 day, animal death occurred. Initial experimental treatment was carried out by i.p. injections at 30 mg/kg every 8 h for 1 day, for a total dose of 90 mg/kg. As illustrated in Fig. 2*A*, DCB-3503 treatment significantly inhibited tumor growth, compared with control animals ($P < 0.0001$). During the first 3 days after treatment, tumor growth was suppressed completely. The body weight dropped to 85% of control on day 5, but returned to normal on day 7 (Fig. 2*B*). DCB-3500 was less active against tumor growth (Fig. 2*A*) and less toxic than DCB-3503, and body weight was very stable after DCB-3500

[5] Hollow-fiber scores were provided to D. C. B. by the Developmental Therapeutics Program/NCI.

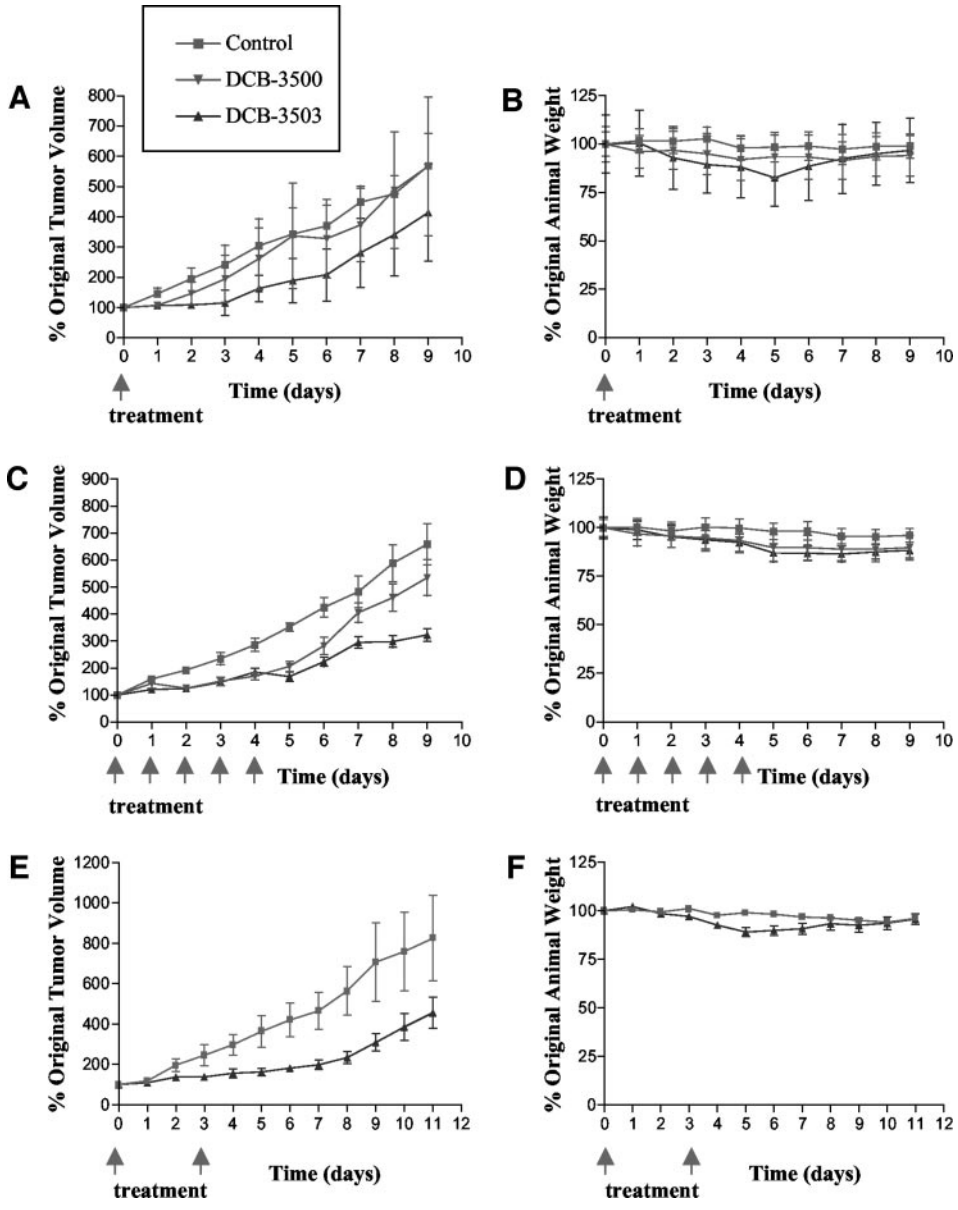

Fig. 2. Inhibition of HepG2 tumor growth by DCB-3500 and DCB-3503. HepG2 cells (8×10^6) were implanted s.c. into nude mice. Treatment was started when the tumors were 100–250 mm^3. Drugs were administered by i.p. injections. *A* and *B*, 30 mg/kg every 8 h on day 0. *C* and *D*, 18 mg/kg/day on days 0–4. *E* and *F*, 6 mg/kg every 8 h on days 0 and 3. *A*, *C*, and *E*, effect of DCB-3500 and/or DCB-3503 on HepG2 tumor growth in nude mice. *B*, *D*, and *F*, effect of DCB-3500 and/or DCB-3503 on the body weight of nude mice. There were five mice in each group. Data points represent the means of the groups; *bars*, SD.

treatment (Fig. 2*B*). To optimize animal treatment protocol, we then tried i.p. injections at 18 mg/kg/day for 5 consecutive days, the same total dose as the above animal experiment. Similarly, DCB-3503 was more active against tumor growth than DCB-3500, tumor growth was suppressed until day 5 (Fig. 2*C*), and body weight loss was <10% (Fig. 2*D*). To further determine the minimal effective dosage for tumor growth suppression, we performed another treatment protocol, by i.p. injections at 3 or 6 mg/kg every 8 h for 1 day, with a total dose of 9 and 18 mg/kg, respectively. Tumor size doubling time for control animals was 2 to ~3 days, and the DCB-3503 treatment (3 or 6 mg/kg, every 8 h for 1 day) group increased the doubling time to 5 to ~6 days (data not shown), suggesting that the effective treatment dosage could be as low as 9 mg/kg for 1 day. On the basis of all of the above results, our next experiment was designed to perform i.p. injections at 6 mg/kg every 8 h on days 0 and 3, with a total dose of 36 mg/kg. With DCB-3503 treatment, tumor growth was suppressed for 7 days (Fig. 2*E*), and a 10% body weight loss was observed on day 5, which returned to normal on day 8 (Fig. 2*F*). The difference in tumor size between the control group and the DCB-3503 treatment group (Fig. 2*E*) was statistically significant (two-way ANOVA was used to compare the tumor size of all time points monitored) at $P < 0.0001$. To summarize, all of the treatment schedules demonstrated that DCB-3503 delayed tumor growth markedly. As shown in Fig. 2, *A*, *C*, and *E*, tumor doubling time for control animals was 2 to ~3 days, whereas for the DCB-3503 treatment group, it was increased to 5 to ~6 days (Fig. 2*A*); 4 days (Fig. 2*C*); or 7 days (Fig. 2*E*). Our data clearly indicate that DCB-3503 has antitumor activity *in vivo* in animals.

Tylophorine and Its Analogs Are Active against Cell Lines Resistant to Some Other Conventional Antitumor Drugs. The activity of all four tylophorine analogs against the KB parental cell line and a number of well-characterized KB-resistant cell lines was studied. The EC_{50}s were similar in KB parental and KB-resistant cell lines as shown in Table 2A. Biochemical changes of each KB-resistant cell line (compared with KB parental cells) and drugs resistant to these cell lines are summarized in Table 2B.

Tylophorine and Its Analogs Do Not Induce p53 Expression. The tumor suppressor protein p53 was shown to be a sensor of DNA damage. Induction of p53 is a key event of cells in response to DNA-damaging agents (34–36). Most chemotherapeutic drugs exert

Table 2 *EC_{50} of DCB-3500, DCB-3501, DCB-3502, and DCB-3503 on the growth inhibition of KB cells and its drug-resistant cells*

A. EC_{50}[a]

Cell line	DCB-3500 (nM)	DCB-3501 (nM)	DCB-3502 (nM)	DCB-3503 (nM)
KB	12 ± 3	106 ± 84	234 ± 91	28 ± 4
KB-MDR[b]	14 ± 5	143 ± 82	282 ± 138	26 ± 8
KB-7D	12 ± 7	225 ± 206	527 ± 80	45 ± 10
KB-7D-Rev	11 ± 6	70 ± 57	289 ± 188	25 ± 10
KB-Hu-R	25 ± 7	70 ± 42	218 ± 167	36 ± 6
KB-Hu-Rev	16 ± 4	45 ± 4	127 ± 95	28 ± 16
KB-100	20 ± 10	103 ± 33	179 ± 63	38 ± 1
KB-100-Rev	10 ± 3	118 ± 31	247 ± 122	41 ± 9

B. Description of resistant cell lines

Cell line	Biochemical changes	Resistant to	Reference
KB-MDR	gp 170 ↑	VP-16, taxol, Adriamycin, vincristine	24
KB-7D	Topo II ↓, MRP ↑	VP-16, vincristine, Adriamycin	25,26
KB-7D-Rev	Topo II ↓	VP-16, Adriamycin	25,26
KB-HU-R	RR ↑, dCK ↓	Hydroxyurea, araC, gemcitabine	27
KB-HU-Rev	dCK ↓	araC, gemcitabine	27
KB-100	Topo I ↓, XRCC 1 ↑	CPT, topotecan, SN-38	28,29
KB-100-Rev	Topo I ↓	CPT, topotecan, SN-38	28

[a] Values are means ± SD of three experiments, with each data point done in triplicate.
[b] MDR, multidrug resistance; MRP, multidrug resistance protein; VP-16, etoposide; HU, hydroxyurea; RR, ribonucleotide reductase; dCK, deoxycytidine kinase; Topo II, topoisomerase II; Topo I, topoisomerase I; XRCC1, X-ray repair cross-complementing gene I protein; araC, arabinoside cytosine; CPT, camptothecin; SN-38, 7-ethyl-10-hydroxycamptothecin.

their antitumor action through DNA damage, resulting in apoptosis. The p53 expression level in response to tylophorine analogs and other conventional antitumor drugs was examined using confocal microscopy and Western blotting. As shown in Fig. 3*A*, p53 induction after treatment with L-OddC, gemcitabine, VP-16, camptothecin (CPT), and hydroxyurea was observed in HepG2 cells, whereas p53 induction was not observed in response to taxol, nocodazole, DCB-3500, and DCB-3503. Taxol and nocodazole are known non-DNA targeting compounds. The same results were obtained using KB cells (data not shown). Expression levels of p53 detected by Western blotting are illustrated in Fig. 3*B*. Expression levels of p21, which is a p53 target gene, were also shown in Fig. 3*B*. Expression of actin was used as an internal control. Changes of p21 correlated with changes of p53. Our results consistently demonstrated that p53 was not induced by DCB-3500 or DCB-3503 treatment (Fig. 3*B, top* and *middle panels, Lanes 2–5*); rather, a decrease of p53 and p21 expression by DCB-3500 and DCB-3503 treatment was observed. L-OddC, CPT, VP-16, and hydroxyurea significantly induced p53 and p21 (Fig. 3*B, top* and *middle panels, Lanes 6–9*). Our data imply that tylophorine analogs do not cause DNA damage as the initial event for their antitumor activity.

Effects of Tylophorine and Its Analogs on Cell Cycle Progression. The impact of tylophorine analogues on cell cycle progression was analyzed using fluorescence-activated cell sorter analysis. KB and HepG2 cells were exposed to 0.03 and 0.3 μM DCB-3500 and 0.3 and 1 μM DCB-3503 for 24 h and subsequently processed for cell cycle analysis. Hydroxyurea and nocodazole were used as positive controls. As shown in Table 3, hydroxyurea induced a G_1-S accumulation, whereas nocodazole induced a G_2-M accumulation in both KB and HepG2 cells. A consistent increase in S-phase was observed in KB cells treated with both DCB-3500 and DCB-3503. Student's *t* test was used to examine the significance of the data. For S-phase in KB cells, values were: 0.03 μM DCB-3500 *versus* control, $P < 0.05$; 0.3 μM DCB-3500 *versus* 0.03 μM DCB-3500, $P < 0.05$; and 0.3 μM DCB-3503 *versus* control, $P < 0.05$. There was no significant difference between 1 μM DCB-3503 and 0.3 μM DCB-3503. We conclude that a dose-dependent S-phase accumulation was observed in KB cells treated with DCB-3500, and S-phase accumulation was also induced with DCB-3503 treatment in KB cells. Surprisingly, no specific cell cycle arrest was observed in HepG2 cells treated with either DCB-3500 or DCB-3503. In view of the potent growth-inhibitory effects of these drugs, we assumed that these drugs equally repressed all phases of the cell cycle of HepG2 cells.

Tylophorine Analogs Do Not Induce Apoptosis in HepG2 Cells. A sub-G_1 content of DNA is typically indicative of apoptosis. On the basis of our cell cycle analysis, no sub-G_1 peak was evident with 1 μM DCB-3500 or DCB-3503 treatment for 24 h in both KB and HepG2 cells. To detect early apoptotic events, the Vybrant apoptosis assay kit from Molecular Probes was used. The purpose of this assay is to distinguish apoptosis from necrosis, if cell death occurs. It can also quantitate three populations of cells with drug treatment: normal viable cells, apoptotic cells, and populations of necrosis. As described in "Materials and Methods," the kit contains Alexa Fluor 488 Annexin V and PI. Annexin V binds various phospholipid species with the highest affinity for phosphatidylserine. In normal cells, phosphatidylserine is situated on the inner leaflet of the plasma membrane. When cell death occurs, phosphatidylserine is translocated to the outer layer of the membrane, *i.e.*, the cell surface. This occurs in the early phases of apoptosis, during which the cell membrane itself remains intact. In contrast, necrosis is accompanied by the loss of cell membrane integrity. PI is usually used to measure cell membrane permeability because of its binding affinity to DNA; therefore, cells that bind only to Annexin V represent early apoptosis. Those undergoing necrosis have affinity for both Annexin V and PI. Negative controls and positive controls were included in these experiments as described in "Materials and Methods." As shown in Fig. 4, normal viable cells are in the *bottom left window*, apoptotic cells are shown in the *bottom right window*, and the population of necrosis is in the *top right window*. Untreated cells yielded only 3% (HepG2) or 5% (KB) apoptotic cells; KB cells treated with 1 μM DCB-3503 for 24 h showed 8% apoptotic cells; and KB cells treated with 3 μM DCB-3503 for 24 h showed 24% apoptotic cells (Fig. 4, *top panel*). In HepG2 cells, 24-h treatment of DCB-3503 at a concentration as high as 3 μM was not associated with significant apoptosis or necrosis (Fig. 4, *bottom panel*). As a control, 10 μM CPT induced 11% apoptosis in HepG2 cells (Fig. 4, *bottom panel*). The CC_{50} of DCB-3503 in HepG2 cells shown in Table 1B, which is much lower than 1 μM, suggests that the suppression of clonogenic ability of HepG2 cells caused by DCB-3503 is unlikely to be attributable to cell death.

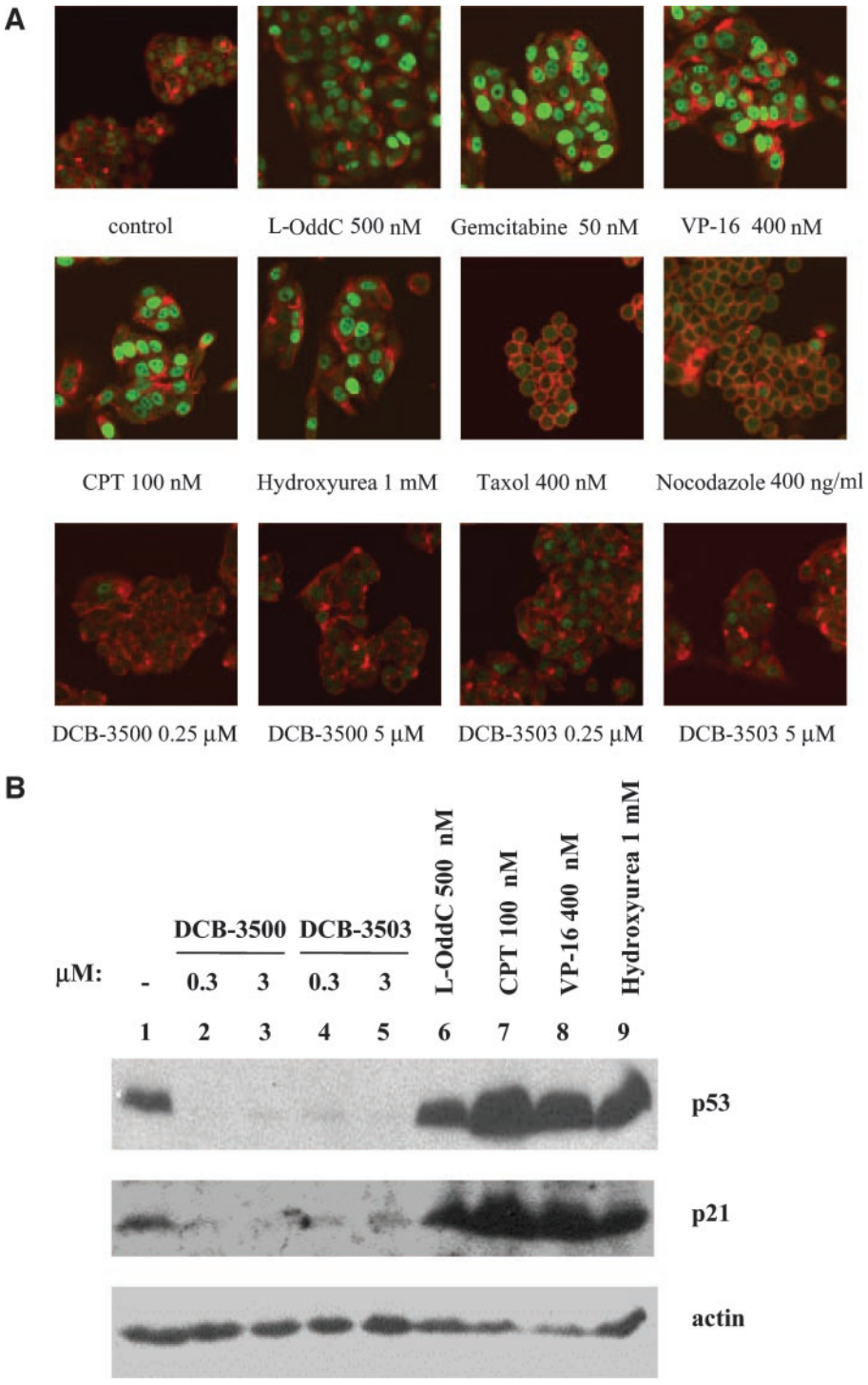

Fig. 3. Changes in p53 and p21 protein levels after treatment with DCB-3500, DCB-3503, and conventional chemotherapeutic drugs. HepG2 cells were treated with conventional anticancer drugs and DCB-3500 and DCB-3503 as indicated for 24 h. *A*, p53 expression level (*green fluorescence*) was probed with specific monoclonal p53 antibody, followed by FITC-conjugated anti-mouse IgG. Cytoplasm (*red fluorescence*) was counterstained with rhodamine phalloidin. Images were obtained by confocal microscopy under the same instrument settings. *B*, p53 and p21 expression was analyzed by Western blot, with actin expression as an internal control.

Effects of Tylophorine and Its Analogs on HepG2 Cell Differentiation. DCB-3500 and DCB-3503 treatment was associated with a morphological change in HepG2 cells. HepG2 cells were treated with 1 μM DCB-3500 or DCB-3503 for 24 h; then drugs were taken away, and the cells were incubated for an additional 3 days. We found that the treated HepG2 cells were vital (trypan blue negative), they did not aggregate like control cells, their cytoplasm portion increased, the cytoplasm:nucleus ratio increased, and the whole cell size increased, resembling a more differentiated phenotype (data not shown). To study whether HepG2 cells became differentiated as a result of DCB-3500 and DCB-3503 treatment, the expression of AFP, a tumor marker, and albumin, a marker of normal hepatocytes, was examined. The relative growth of HepG2 cells in response to 24-h exposure to tylophorine analogs is shown in Fig. 5*A*; DCB-3500 treatment resulted in complete cell growth inhibition. On days 2, 4, 6, and 8, control cells grew rapidly with a high level expression of AFP (Fig. 5*B, upper panel*); 1 μM DCB-3500 24-h treatment resulted a significant down-regulation of AFP expression (Fig. 5*B, lower panel*). On the other hand, albumin expression was up-regulated on day 5 (Fig. 5*C, lower panel*) after DCB-3500 treatment; KB cells were negative control (Fig. 5*C, upper panel*). These changes are consistent with differentiation of HepG2 cells.

Table 3 *DCB-3500 and DCB-3503 induce S-phase accumulation in KB cells but not in HepG2 cells*

KB and HepG2 cells were treated with two concentrations of DCB-3500 and DCB-3503 for 24 h. At the end of treatment, cells were washed, resuspended in PBS, and stained with PI containing RNase A for flow cytometric analysis. Data were analyzed using Modfit software. Results are means ± SD of three independent experiments. Student's *t* test was used to examine the significance of the data. For S phase in KB cells, 0.03 μM DCB-3500 *versus* control, $P < 0.05$; 0.3 μM DCB-3500 *versus* 0.03 μM DCB-3500, $P < 0.05$; 0.3 μM DCB-3503 *versus* control, $P < 0.05$; but there was no significant difference between 1 μM DCB-3503 and 0.3 μM DCB-3503.

	KB			HepG2		
	G_0–G_1 (%)	S (%)	G_2–M (%)	G_0–G_1 (%)	S (%)	G_2–M (%)
Control	68 ± 10	12 ± 5	19 ± 5	46 ± 4	25 ± 9	29 ± 5
Hydroxyurea 2 mM	70 ± 7	26 ± 1	9 ± 5	49 ± 10	33 ± 17	19 ± 10
Nocodazole 0.1 μg/ml	6 ± 3	14 ± 3	81 ± 10	4 ± 3	13 ± 8	83 ± 10
DCB-3500 0.03 μM	62 ± 1	21 ± 4	16 ± 4	45 ± 5	24 ± 8	31 ± 6
DCB-3500 0.3 μM	55 ± 9	32 ± 6	12 ± 6	55 ± 5	17 ± 6	25 ± 5
DCB-3503 0.3 μM	59 ± 7	24 ± 7	18 ± 3	52 ± 4	22 ± 4	25 ± 6
DCB-3503 1 μM	63 ± 1	24 ± 1	13 ± 1	50 ± 8	21 ± 8	29 ± 2

Effects of Tylophorine and Its Analogs on Key Signaling Pathways. The impact of tylophorine analogs on several key signaling pathways was studied by using the Mercury Pathway Profiling System (Clontech), which consists of several promoter-reporter plasmids. These plasmids contained the luciferase reporter gene downstream of several copies of specific transcription factor binding sequences such as activator protein-1 (AP-1), cAMP response element (CRE), and NF-κB. Transcriptional activity of luciferase reporter genes under the control of transcription factor AP-1, CRE-binding protein, and NF-κB were analyzed using transient transfection. As shown in Fig. 6, DCB-3500 had an inhibitory effect on all three signaling pathways in a dose-dependent manner. TPA, forskolin, and TNF-α were used as activators of AP-1, CRE, and NF-κB, respectively. AP-1 activation induced by TPA was ~3-fold (Fig. 6*A*, compare *Lane 9* to *Lane 1*); DCB-3500 inhibited not only TPA-potentiated AP-1 activation (Fig. 6*A*, compare *Lanes 13–16* to *Lane 9*) but also endogenous AP-1 activity (Fig. 6*A*, compare *Lanes 5–8* to *Lane 1*). This inhibitory effect on endogenous AP-1 activity can be explained by the relatively high levels of expression of AP-1 transcription factors in HepG2 cells. As shown in Fig. 6*B*, CRE activation by forskolin was >10-fold (compare *Lane 9* to *Lane 1*). The inhibitory concentration of CRE by DCB-3500 is similar to that of AP-1. In Fig. 6*C*, NF-κB activation by TNF-α was ~10-fold (compare *Lane 9* to *Lane 1*). The inhibition of NF-κB by DCB-3500 was more potent than AP-1 and CRE. The IC_{50} (50% inhibitory concentration) of DCB-3500 for AP-1 and CRE is around 500 nM, and that for NF-κB is 30 nM, representing a 16-fold difference. To avoid the possible artifact of transient transfection attributable to using a transfection reagent and to further confirm the potent inhibitory effect of tylophorine analogs on NF-κB, stable transfectants carrying NF-κB reporter vector were generated. When the inhibition of NF-κB by DCB-3503 was examined, the IC_{50} was found to be 100 nM (Fig. 6*D*). We also examined whether DCB-3503 had an inhibitory effect on mitogen-activated protein kinase ERK1/2 activity. ERK1/2 activity was analyzed by Western blotting using a specific phospho-ERK1/2 antibody. U0126, which is a known MEK1/2 (upstream of ERK1/2) inhibitor, was used as a positive control. Total ERK1/2 activity was used as internal control. As shown in Fig. 6*E*, 10 ng/ml TPA treatment alone (*Lane 2*) markedly induced the ERK1/2 phosphorylation level, and DCB-3503 (*Lanes 3–5*) had no inhibitory effect on TPA-induced ERK 1/2 phosphorylation, in contrast U0126 (*Lane 6*) exerted a potent inhibitory effect on ERK 1/2 phosphorylation. These data indicate that DCB-3503 is not an ERK1/2 inhibitor.

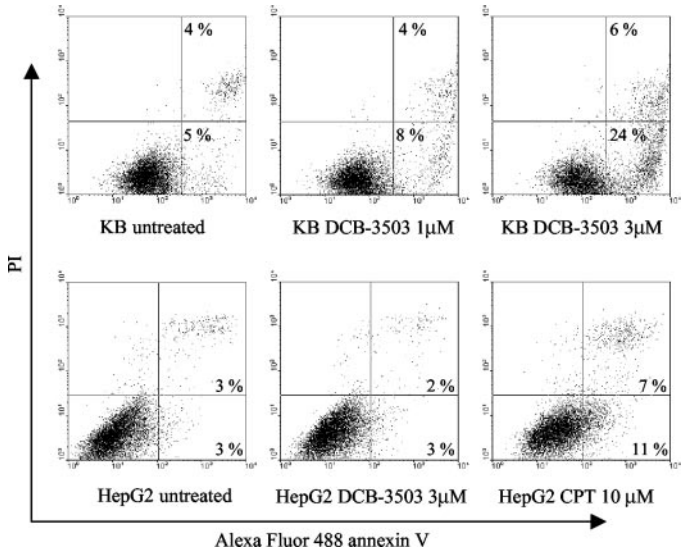

Fig. 4. DCB-3503 does not induce apoptosis in HepG2 cells. Untreated or DCB-3503-treated KB and HepG2 cells (2×10^6) were stained with Alexa Fluor 488 Annexin V and PI and were analyzed by flow cytometer. The percentage of apoptotic cells (*lower right panel*) and necrotic population (*upper right panel*) is shown. CPT, a known apoptosis-inducing agent, was used as a positive control. Experiments were reproduced three times, and one typical experiment is shown.

DISCUSSION

Novel Antitumor Action of Tylophorine Analogs. Novel antitumor chemotherapeutic drugs with different modes of action are needed for the treatment of patients with cancer, particularly those refractory to standard treatment. Tylophorine compounds were shown to have a unique spectrum of activity in comparison with current antitumor drugs based on NCI tumor cell panel studies. This class of compounds has a novel chemical structure in comparison with other antitumor drugs. The antitumor potential of these compounds in the animal models has not been studied before, and their mode of action is currently unknown. Many antitumor drugs exert action by targeting DNA synthesis or inducing DNA damage, consequently resulting in cell cycle perturbations and apoptosis. To elucidate the mechanism of action of the tylophorine analogs, we first examined whether these compounds can induce DNA damage; because p53 is a sensor of DNA damage (34–36), we investigated the changes of p53 in response to tylophorine analog treatment. Activation of p53 triggers apoptosis or DNA repair. In addition, p53 activation has also been implicated in triggering cell cycle arrest, including both the G_1 and G_2 phases of the cell cycle (34). The mechanism of cell cycle arrest within the G_1 phase of the cell cycle is understood by p53 stimulating transcription of the gene for the cyclin-dependent kinase inhibitory protein p21. Elevated levels of p21 then inhibit the cyclin E/cyclin-dependent kinase 2 and cyclin A/cyclin-dependent kinase 2 kinases, thus preventing these kinases from promoting cell cycle progression (34). As shown in Fig. 2, DCB-3500 and DCB-3503 both failed to induce p53. Consistently, these drugs also did not elevate expression of p21. However, under the same experimental conditions, both p53 and p21 were induced by

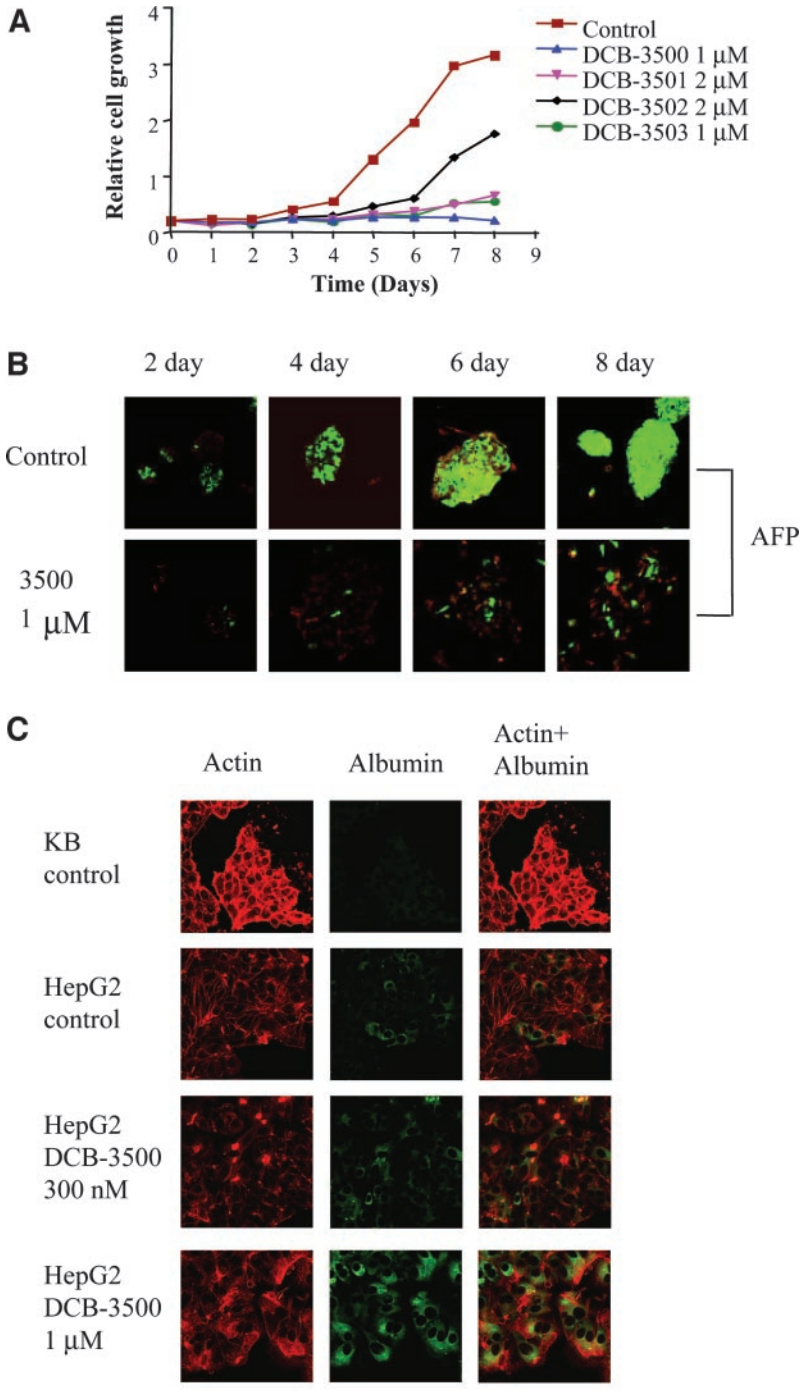

Fig. 5. Regulation of AFP and albumin expression by DCB-3500 in HepG2 cells. *A*, growth-inhibitory effect of tylophorine analogs in HepG2 cells. HepG2 cells were treated with DCB-3500, DCB-3501, DCB-3502, and DCB-3503 as indicated for 24 h; then the drugs were taken away, and cell growth was monitored by methylene blue staining. *B*, HepG2 cells were treated with or without DCB-3500 for 24 h, and then the drug was taken away. On days 2, 4, 6, and 8, AFP expression (*green fluorescence*) was monitored by confocal microscopic analysis using an anti-AFP antibody. Actin (*red fluorescence*) was counterstained. *C*, HepG2 cells were treated with or without DCB-3500 as indicated for 24 h, and then the drug was taken away. On day 5, albumin expression (*green fluorescence*) was detected by confocal microscopy using an anti-albumin antibody.

L-OddC, VP-16, CPT, and hydroxyurea treatment in HepG2 cells (Fig. 3). Although an S-phase accumulation by DCB-3500 and DCB-3503 treatment was observed in KB cells, we failed to detect the same or other cell cycle effects in HepG2 cells. Furthermore, apoptosis was not induced by 3 μM DCB-3503 treatment in HepG2 cells (Fig. 4). Our preliminary studies also failed to detect senescence-associated β-galactosidase expression with DCB-3500 treatment in HepG2 cells (data not shown). Because these compounds are very potent against all of the cell lines we tested including drug-resistant cell lines (EC_{50}, $\sim 10^{-8}$ M), we are very much intrigued by their mechanism of action. This led us to consider the possibility of differentiation. Indeed, the morphological changes, up-regulation of AFP, and down-regulation of albumin support the direction of differentiation. However, our data do not exclude other yet-unidentified mechanisms of antitumor action.

HCC is refractory to chemotherapy because of tumor heterogeneity, the development of multidrug resistance phenotypes, and recently reported constitutive expression of NF-κB (37). A successful anticancer drug for the treatment of HCC would, therefore, overcome at least some of these resistance mechanisms. The activity of tylophorine analogs against resistant cell lines and the lack of cross-resistance with other conventional anticancer drugs as indicated in Table 2 imply that this class of compounds may use a novel mechanism for their

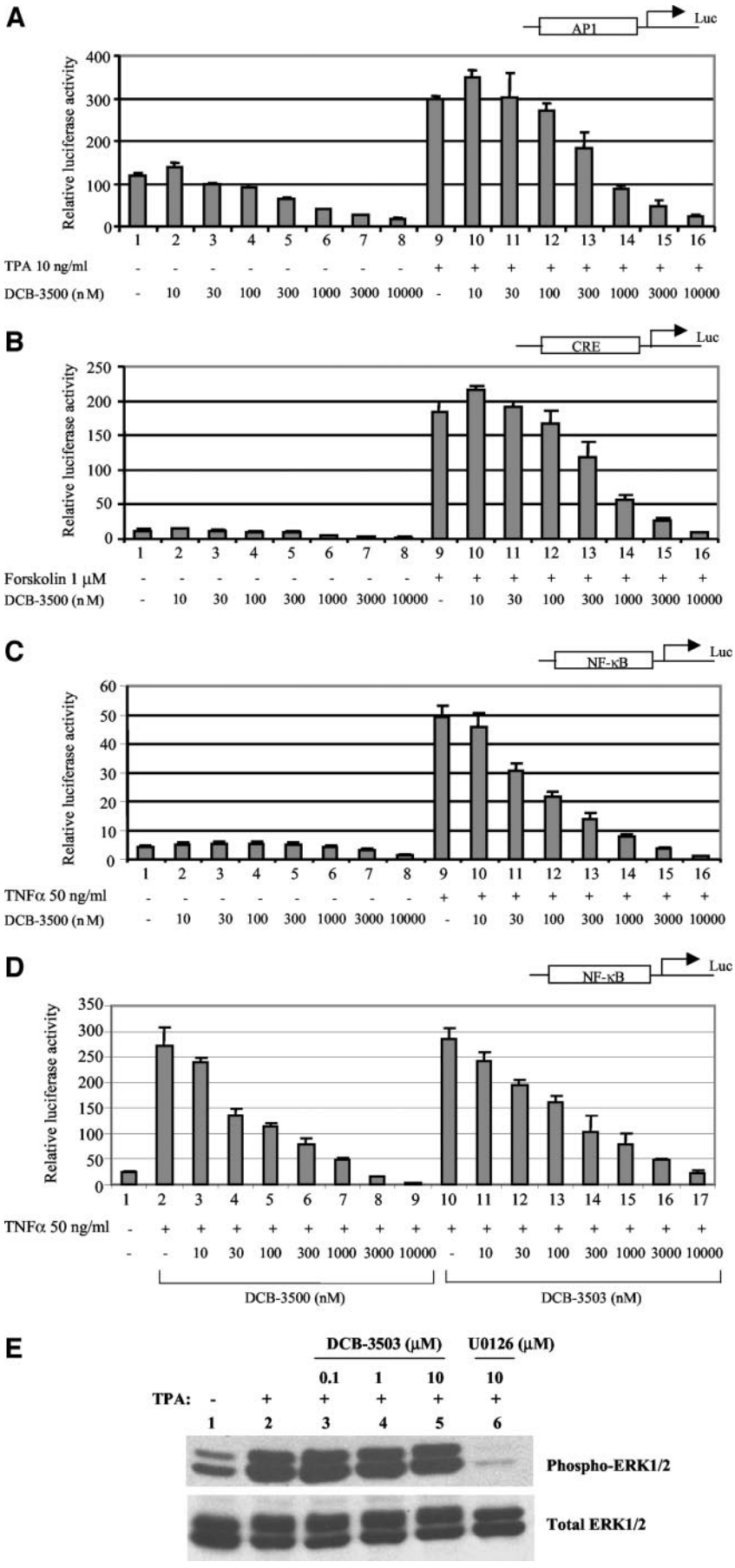

Fig. 6. Inhibition of key signaling pathways by DCB-3500 and/or DCB-3503. HepG2 cells were transiently transfected with firefly luciferase reporter vectors pAP1-luc (*A*), pCRE-luc (*B*), or pBIIX-luc (*C*), along with an internal control vector phRL-luc, which is a promoterless *Renilla* luciferase reporter vector. The day after transfection, cells were pretreated with increasing concentrations of DCB-3500 for 1 h and then stimulated with TPA, forskolin, or TNF-α as indicated for 4 h. Firefly and *Renilla* luciferase activities were measured using Promega's dual-luciferase assay kit. Data shown was firefly luciferase activity. *D*, HepG2 cells stably transfected with pBIIX-luc were pretreated with increasing concentrations of DCB-3500 or DCB-3503 for 1 h, and then cells were stimulated with TNF-α for 4 h. Luciferase activities were measured using Promega's luciferase assay kit. Luciferase activity is reported as relative activity from a single representative experiment ($n = 3$ independent transfections/treatment); *bars*, SE. All transfection studies were conducted on at least three separate occasions with similar results. *E*, HepG2 cells were serum starved for 24 h and pretreated with DCB-3503 or MEK1/2 inhibitor U0126 (Cell Signaling Technology) as indicated for 1 h; cells were then stimulated with 10 ng/ml TPA for 15 min. Whole-cell extracts were probed with specific phospho-ERK1/2 and -ERK1/2 antibody. A representative Western blot is shown.

antitumor activity and may target a novel protein. Their potential in combination chemotherapy with conventional antitumor agents will be explored in the future.

Potency and Selectivity of Tylophorine Analogs. In the late 1960s, some tylophorine analogs were evaluated at the NCI, among them both enantiomers of tylophorine, but none were deemed interesting enough to warrant further research. In the 1990s, some related analogs in this class of compounds were again screened for antitumor potential by the NCI using NCI's 60-tumor cell line panel. The drugs initially studied were tyloindicine F (NSC-650393), tyloindicine G (NSC-650394), tyloindicine H (NSC-650395), and tyloindicine I (NSC-650396). Among these, tyloindicine F and tyloindicine G showed very potent and uniform activity against 54 human tumor cell lines with $GI_{50} < 10^{-10}$ M, ranked as the number 1 and number 2, respectively, most potent antitumor agents examined in a screen that included 33,744 compounds (data not shown). Moreover, tyloindicine F and tyloindicine G were quite selective toward some melanoma and lung cancer cell lines based on LC_{50}s. The LC_{50}s for several of the melanoma and lung cancer cell lines were two orders of magnitude less than those for the other cell lines (data not shown). Tyloindicine F and tyloindicine G are not readily available from their natural sources; thus, they are our future goals of synthesis. The four related tylophorine analogs used in our present study were originally synthesized to study structure-activity relationships, yet they showed potent growth inhibition. On the basis of the NCI study with DCB-3500 and DCB-3503, the GI_{50} is around 10^{-8} M against 60 human tumor cell lines.[3] From our studies, the EC_{50}s of DCB-3500 and DCB-3503 against KB, KB-resistant cell lines, HepG2, SK-Hep1, Huh7, PLC/PRF5, Hep3B, HA22T, and Mahlavu is also around 10^{-8} M, which is very close to most currently used antitumor drugs such as CPT and gemcitabine. We then examined their *in vivo* antitumor potential.

In addition to the potency against cell growth, using HepG2 and KB human tumor cell lines, we demonstrated that HepG2 cells were more sensitive to tylophorine analogs in terms of loss of clonogenic ability; the CC_{50} of HepG2 is 10-fold less than KB, as shown in Table 1. Moreover, the cell cycle effects of these drugs were different in KB and HepG2 cells, as illustrated in Table 3. These differential effects of the cell lines in response to these drugs raised the possibility that tylophorine analogs could selectively inhibit certain tumor growth. In addition to the novel mechanism of action of the tylophorine analogs, their potency and selectivity against certain cancers dictate that further exploration of the antitumor potential of these compounds is required.

Discrepancy of Tylophorine Analogs *in Vitro* and *in Vivo*. In our animal studies, we found that the growth of tumor xenografts was markedly suppressed by treatment with DCB-3503. To our surprise, DCB-3500 was less active than DCB-3503 *in vivo*, despite the fact that data on *in vitro* cell growth inhibition showed that DCB-3500 was the most potent among the four tylophorine analogs we tested. This could be attributable to the difference of pharmacokinetics between these drugs, and this point will be investigated. On the basis of this discrepancy of *in vitro* and *in vivo* data, we cannot exclude the possibility that DCB-3501 or DCB-3502 may have a better therapeutic index than DCB-3500 against certain types of cancer such as HCC. *In vivo* study of these two drugs should be performed as well. Furthermore, additional tylophorine analogs will be synthesized and screened for antitumor activity both *in vitro* and *in vivo*.

Potent Inhibition of NF-κB-Mediated Transcription by Tylophorine Analogs. Tylophorine and some analogs were synthesized as early as 1960 (38), and their inhibition of protein and nucleic acid synthesis has been documented (2, 4). A comprehensive evaluation of their antitumor potential has not been reported, and mechanisms of growth inhibition are largely unknown. A systematic investigation and analysis of the mechanism and mode of action of this class of compounds may facilitate discovery of a novel anticancer target. In addition to investigating the effects of tylophorine analogs on the cell cycle, apoptosis, and differentiation, the effects of these drugs on modulation of transcriptional activity of some transcription factors were also studied, because signaling pathways and transcription factors have been proposed recently as important anticancer targets (19, 20, 39). We focused on the activator protein-1, the CRE, and the NF-κB signaling pathways, because these pathways have been well studied and are important players in the control of cell growth, differentiation, and survival (39, 40). We found that DCB-3500 could significantly inhibit activator protein-1-, CRE-, and NF-κB-mediated transcription. Most remarkably, 30 nM DCB-3500 and 100 nM DCB-3503 exerted a 50% inhibition on NF-κB-mediated transcription. Our data also showed that the activity of mitogen-activated protein kinase ERK1/2 is not affected by DCB-3503 treatment (Fig. 6*E*). Whether the inhibition of these transcription factor families activator protein-1 and CRE-binding protein could be attributable to the crosstalk among these signaling pathways and NF-κB or independent events is not clear. This point will be investigated further. In addition, the potent action of this class of compounds on other cellular targets could also be possible. However, our results imply that tylophorine analogs may alter the activity of above transcription factors, subsequently modulating the expression of their target genes involved in the control of cell growth, differentiation, and survival.

In conclusion, we have demonstrated that tylophorine analogs are active against HepG2 tumor cells both *in vitro* and *in vivo*, with a unique mode of action different from other known antitumor compounds. The results reported herein may suggest potential clinical application of tylophorine and its analogs against cancer, especially for those refractory to current chemotherapy.

ACKNOWLEDGMENTS

We acknowledge Rocco Carbone and Yashang Lee for technical assistance in cell cycle analysis; Zaoli Jiang for assistance with the tumor xenograft model; and Tracey Kim and Elizabeth Gullen for critical reading of the manuscript.

REFERENCES

1. Li, Z., Zhong, J., and Huang, R. Isolation, total synthesis and biological activity of phenanthroindolizidine and phenanthroquinolizidine alkaloids. Synthesis, *16:* 2365–2378, 2001.
2. Donaldson, G. R., Atkinson, M. R., and Murray, A. W. Inhibition of protein synthesis in Ehrlich ascites-tumour cells by the phenanthrene alkaloids tylophorine, tylocrebrine and cryptopleurine. Biochem. Biophys. Res. Commun., *31:* 104–109, 1968.
3. Rao, K. V., Wilson, R. A., and Cummings, B. Alkaloids of tylophora. III. New alkaloids of *Tylophora indica* (Burm) Merrill and *Tylophora dalzellii* Hook. f. J. Pharm. Sci., *60:* 1725–1726, 1971.
4. Rao, K. N., Bhattacharya, R. K., and Venkatachalam, S. R. Inhibition of thymidylate synthase and cell growth by the phenanthroindolizidine alkaloids pergularinine and tylophorinidine. Chem. Biol. Interact., *106:* 201–212, 1997.
5. Rao, K. N., and Venkatachalam, S. R. Inhibition of dihydrofolate reductase and cell growth activity by the phenanthroindolizidine alkaloids pergularinine and tylophorinidine: the *in vitro* cytotoxicity of these plant alkaloids and their potential as antimicrobial and anticancer agents. Toxicol. Vitro, *14:* 53–59, 2000.
6. Staerk, D., Lykkeberg, A. K., Christensen, J., Budnik, B. A., Abe, F., and Jaroszewski, J. W. *In vitro* cytotoxic activity of phenanthroindolizidine alkaloids from *Cynanchum vincetoxicum* and *Tylophora tanakae* against drug-sensitive and multidrug-resistant cancer cells. J. Nat. Prod., *65:* 1299–1302, 2002.
7. Ganguly, T., and Khar, A. Induction of apoptosis in a human erythroleukemic cell line K562 by tylophora alkaloids involves release of cytochrome *c* and activation of caspase 3. Phytomedicine, *9:* 288–295, 2002.
8. Komatsu, H., Watanabe, M., Ohyama, M., Enya, T., Koyama, K., Kanazawa, T., Kawahara, N., Sugimura, T., and Wakabayashi, K. Phenanthroindolizidine alkaloids as cytotoxic substances in a Danaid butterfly, *Ideopsis similis*, against human cancer cells. J. Med. Chem., *44:* 1833–1836, 2001.
9. Paull, K. D., Hamel, E., and Malspeis, L. Prediction of biochemical mechanism of action from the *in vitro* antitumor screen of the National Cancer Institute. *In:* W. O. Foye (ed.), Cancer Chemotherapeutic Agents, pp. 9–45. Washington, DC: American Chemical Society, 1995.

10. El-Serag, H. B., and Mason, A. C. Rising incidence of hepatocellular carcinoma in the United States. N. Engl. J. Med., *340:* 745–750, 1999.
11. McCaughan, G. W., Koorey, D. J., and Strasser, S. I. Hepatocellular carcinoma: current approaches to diagnosis and management. Intern. Med. J., *32:* 394–400, 2002.
12. Juliano, R. L., and Ling, V. A surface glycoprotein modulating drug permeability in Chinese hamster ovary cell mutants. Biochim. Biophys. Acta, *455:* 152–162, 1976.
13. Gerlach, J. H., Endicott, J. A., Juranka, P. F., Henderson, G., Sarangi, F., Deuchars, K. L., and Ling, V. Homology between P-glycoprotein and a bacterial haemolysin transport protein suggests a model for multidrug resistance. Nature (Lond.), *324:* 485–489, 1986.
14. Cole, S. P., Bhardwaj, G., Gerlach, J. H., Mackie, J. E., Grant, C. E., Almquist, K. C., Stewart, A. J., Kurz, E. U., Duncan, A. M., and Deeley, R. G. Overexpression of a transporter gene in a multidrug-resistant human lung cancer cell line. Science (Wash. DC), *258:* 1650–1654, 1992.
15. Xu, Y., and Villalona-Calero, M. A. Irinotecan: mechanisms of tumor resistance and novel strategies for modulating its activity. Ann. Oncol., *13:* 1841–1851, 2002.
16. Beck, W. T., Morgan, S. E., Mo, Y. Y., and Bhat, U. G. Tumor cell resistance to DNA topoisomerase II inhibitors: new developments. Drug Resist. Updat., *2:* 382–389, 1999.
17. Wang, C. Y., Cusack, J. C., Jr., Liu, R., and Baldwin, A. S., Jr. Control of inducible chemoresistance: enhanced anti-tumor therapy through increased apoptosis by inhibition of NF-κB. Nat. Med., *5:* 412–417, 1999.
18. Cusack, J. C., Jr., Liu, R., and Baldwin, A. S., Jr. Inducible chemoresistance to 7-ethyl-10-[4-(1-piperidino)-1-piperidino]-carbonyloxycamptothecin (CPT-11) in colorectal cancer cells and a xenograft model is overcome by inhibition of nuclear factor-κB activation. Cancer Res., *60:* 2323–2330, 2000.
19. Manley, P. W., Cowan-Jacob, S. W., Buchdunger, E., Fabbro, D., Fendrich, G., Furet, P., Meyer, T., and Zimmermann, J. Imatinib: a selective tyrosine kinase inhibitor. Eur. J. Cancer, *38:* S19–S27, 2002.
20. Gilmore, T., Gapuzan, M. E., Kalaitzidis, D., and Starczynowski, D. Rel/NF-κB/IκB signal transduction in the generation and treatment of human cancer. Cancer Lett., *181:* 1–9, 2002.
21. Sen, R., and Baltimore, D. Multiple nuclear factors interact with the immunoglobulin enhancer sequences. Cell, *46:* 705–716, 1986.
22. Bharti, A. C., and Aggarwal, B. B. Nuclear factor-κB and cancer: its role in prevention and therapy. Biochem. Pharmacol., *64:* 883–888, 2002.
23. Mitchell, B. S. The proteasome–an emerging therapeutic target in cancer. N. Engl. J. Med., *348:* 2597–2598, 2003.
24. Chen, H. X., Bamberger, U., Heckel, A., Guo, X., and Cheng, Y. C. BIBW 22, a dipyridamole analogue, acts as a bifunctional modulator on tumor cells by influencing both P-glycoprotein and nucleoside transport. Cancer Res., *53:* 1974–1977, 1993.
25. Ferguson, P. J., Fisher, M. H., Stephenson, J., Li, D. H., Zhou, B. S., and Cheng, Y. C. Combined modalities of resistance in etoposide-resistant human KB cell lines. Cancer Res., *48:* 5956–5964, 1988.
26. Gaj, C. L., Anyanwutaku, I., Chang, Y. H., and Cheng, Y. C. Decreased drug accumulation without increased drug efflux in a novel MRP-overexpressing multi-drug-resistant cell line. Biochem. Pharmacol., *55:* 1199–1211, 1998.
27. Yen, Y., Grill, S. P., Dutschman, G. E., Chang, C. N., Zhou, B. S., and Cheng, Y. C. Characterization of a hydroxyurea-resistant human KB cell line with supersensitivity to 6-thioguanine. Cancer Res., *54:* 3686–3691, 1994.
28. Beidler, D. R., Chang, J. Y., Zhou, B. S., and Cheng, Y. C. Camptothecin resistance involving steps subsequent to the formation of protein-linked DNA breaks in human camptothecin-resistant KB cell lines. Cancer Res., *56:* 345–353, 1996.
29. Park, S. Y., Lam, W., and Cheng, Y. C. X-ray repair cross-complementing gene I protein plays an important role in camptothecin resistance. Cancer Res., *62:* 459–465, 2002.
30. Finlay, G. J., Baguley, B. C., and Wilson, W. R. A semiautomated microculture method for investigating growth inhibitory effects of cytotoxic compounds on exponentially growing carcinoma cells. Anal. Biochem., *139:* 272–277, 1984.
31. Buckley, T. F., and Rapoport, H. α-Amino acids as chiral educts for asymmetric products. Chirally specific syntheses of tylophorine and cryptopleurine. J. Org. Chem., *48:* 4222–4232, 1983.
32. Hollingshead, M. G., Alley, M. C., Camalier, R. F., Abbott, B. J., Mayo, J. G., Malspeis, L., and Grever, M. R. *In vivo* cultivation of tumor cells in hollow fibers. Life Sci., *57:* 131–141, 1995.
33. Plowman, J., Dykes, D. J., Hollingshead, M., Simpson-Herren, L., and Alley, M. C. Human tumor xenograft models in NCI drug development. *In:* B. Teicher (ed), Anticancer Drug Development Guide: Preclinical Screening, Clinical Trials, and Approval, pp. 101–125. Totowa, NJ: Humana Press, 1997.
34. Lakin, N. D., and Jackson, S. P. Regulation of p53 in response to DNA damage. Oncogene, *18:* 7644–7655, 1999.
35. Milner, J. DNA damage, p53 and anticancer therapies. Nat. Med., *1:* 879–880, 1995.
36. Wahl, G. M., and Carr, A. M. The evolution of diverse biological responses to DNA damage: insights from yeast and p53. Nat. Cell. Biol., *3:* E277–E286, 2001.
37. Tai, D. I., Tsai, S. L., Chang, Y. H., Huang, S. N., Chen, T. C., Chang, K. S., and Liaw, Y. F. Constitutive activation of nuclear factor κB in hepatocellular carcinoma. Cancer (Phila.), *89:* 2274–2281, 2000.
38. Govindachari, T. R., Lakshmikantham, M. V., and Rajadurai, S. Synthesis of (+/−)-tylophorine. Chem. Ind. (Lond.), *23:* 664–664, 1960.
39. Darnell, J. E., Jr. Transcription factors as targets for cancer therapy. Nat. Rev. Cancer, *2:* 740–749, 2002.
40. Shaulian, E., and Karin, M. AP-1 as a regulator of cell life and death. Nat. Cell Biol., *4:* E131–E136, 2002.